Çatalhöyük Excavations: The 2009–2017 Seasons

Edited by

Ian Hodder

Colour & scalable figures for Chapter 4. Geophysical survey at Çatalhöyük: results of combined magnetometer and ground penetrating radar

Kristian Strutt, Stefano Campana, Jessica Ogden,
Gianluca Catanzariti and Gianfranco Morelli

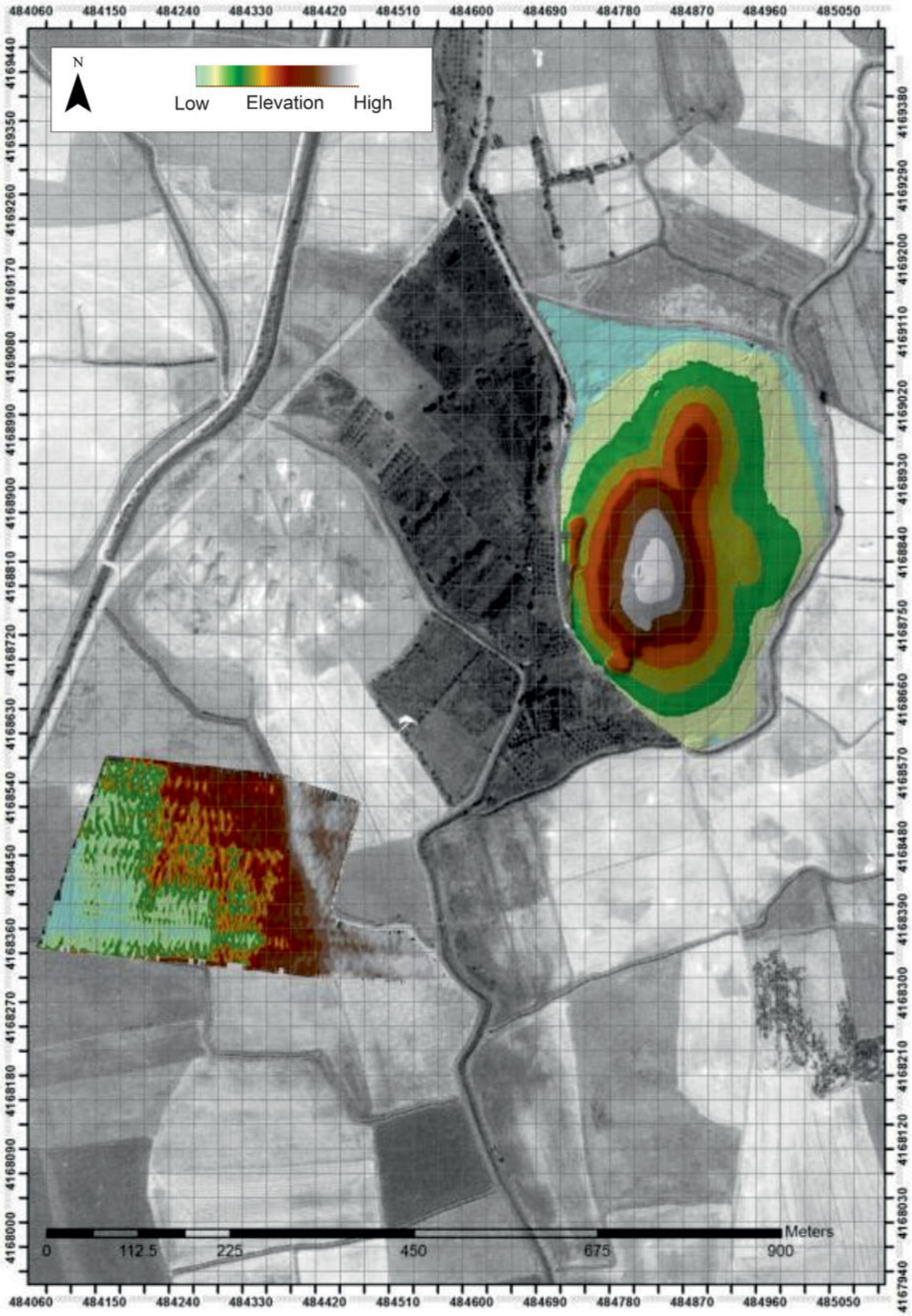

Figure 4.2. The East Mound in relation to the topographic survey conducted in 2012 in UTM 36N.

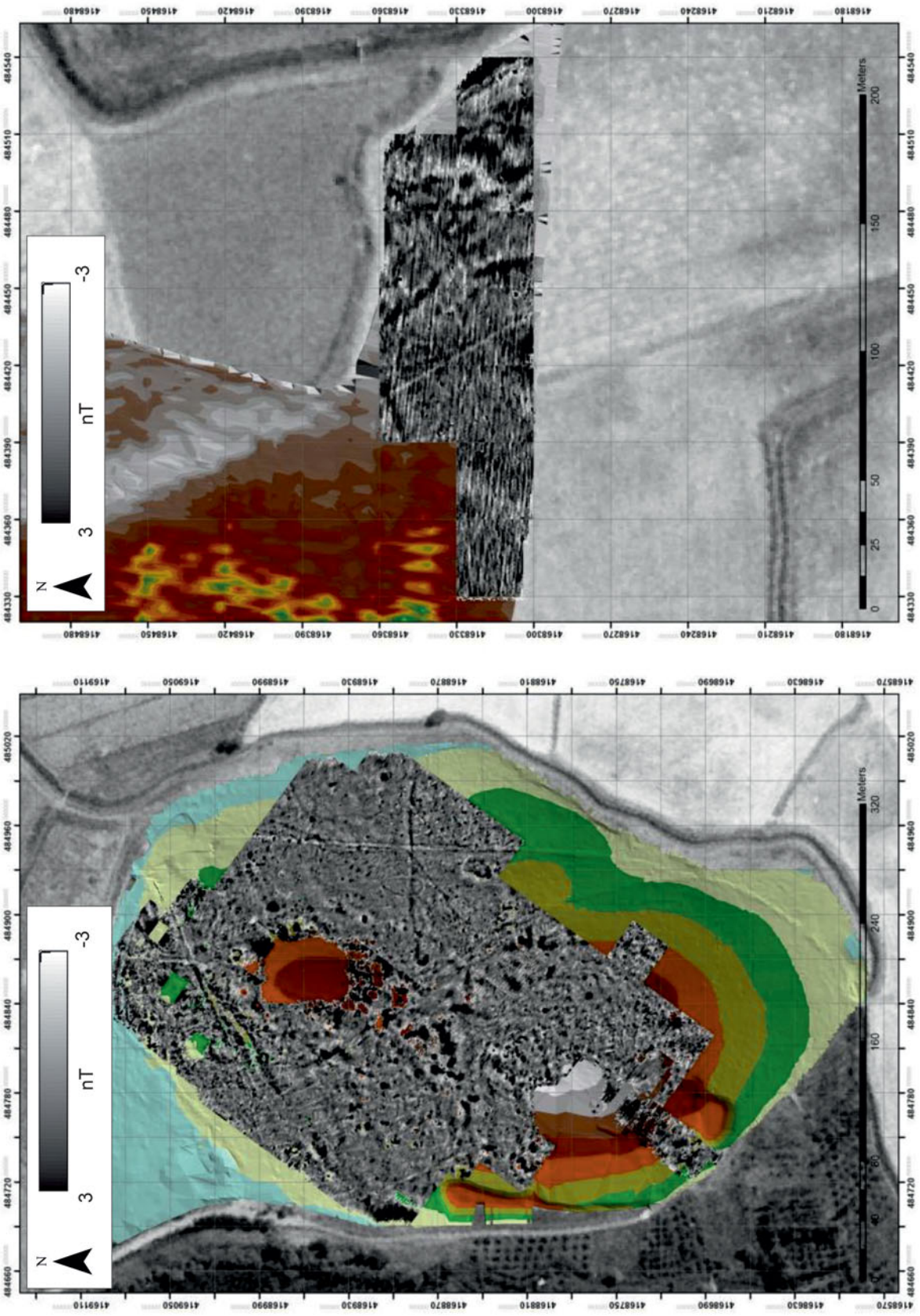

Figure 4.3. The results of the magnetometer survey for the East Mound (left) and in the fields (right) overlaid onto the topographic survey.

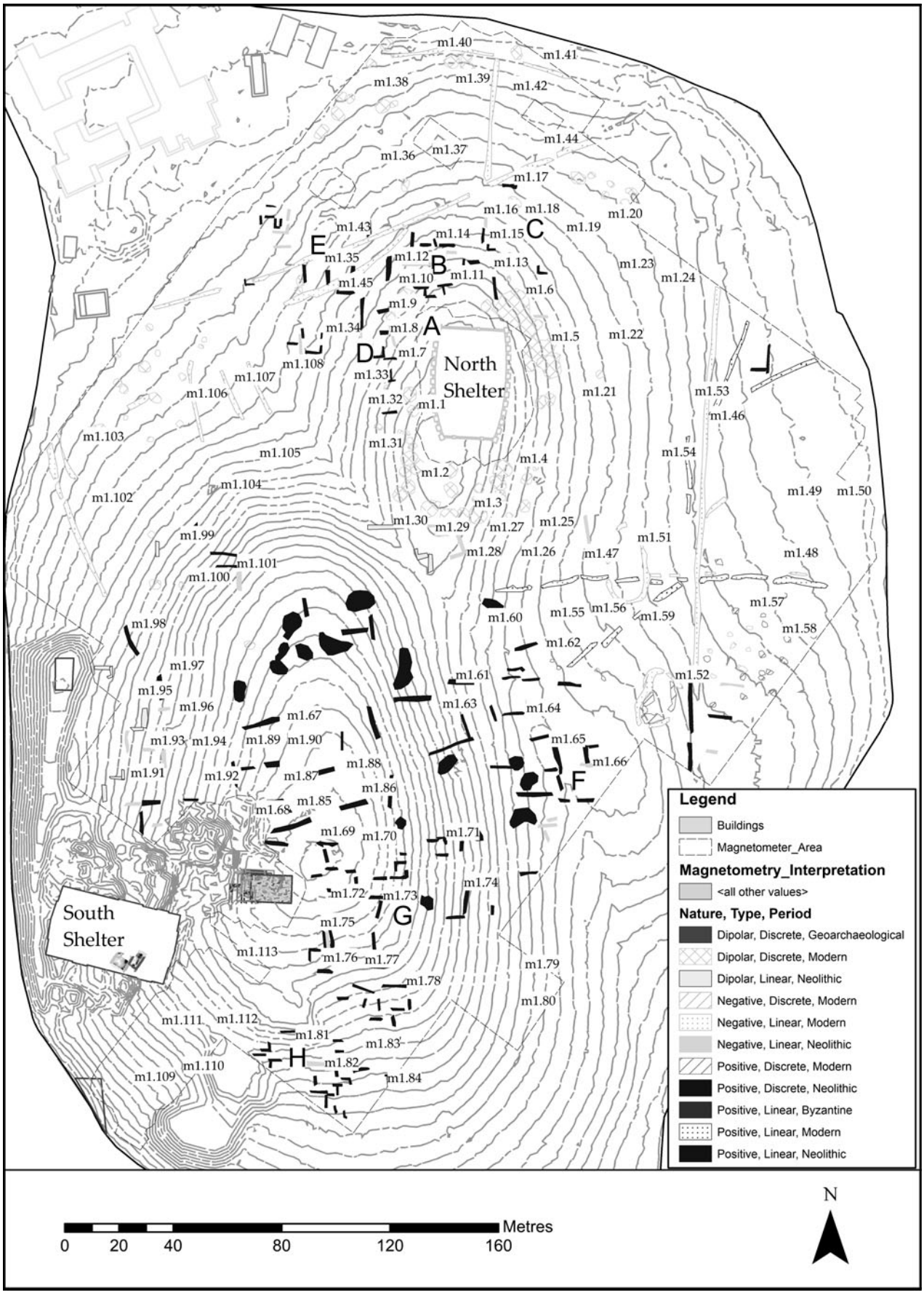

Figure 4.4. Interpretation plot derived from the magnetometer survey for the East Mound.

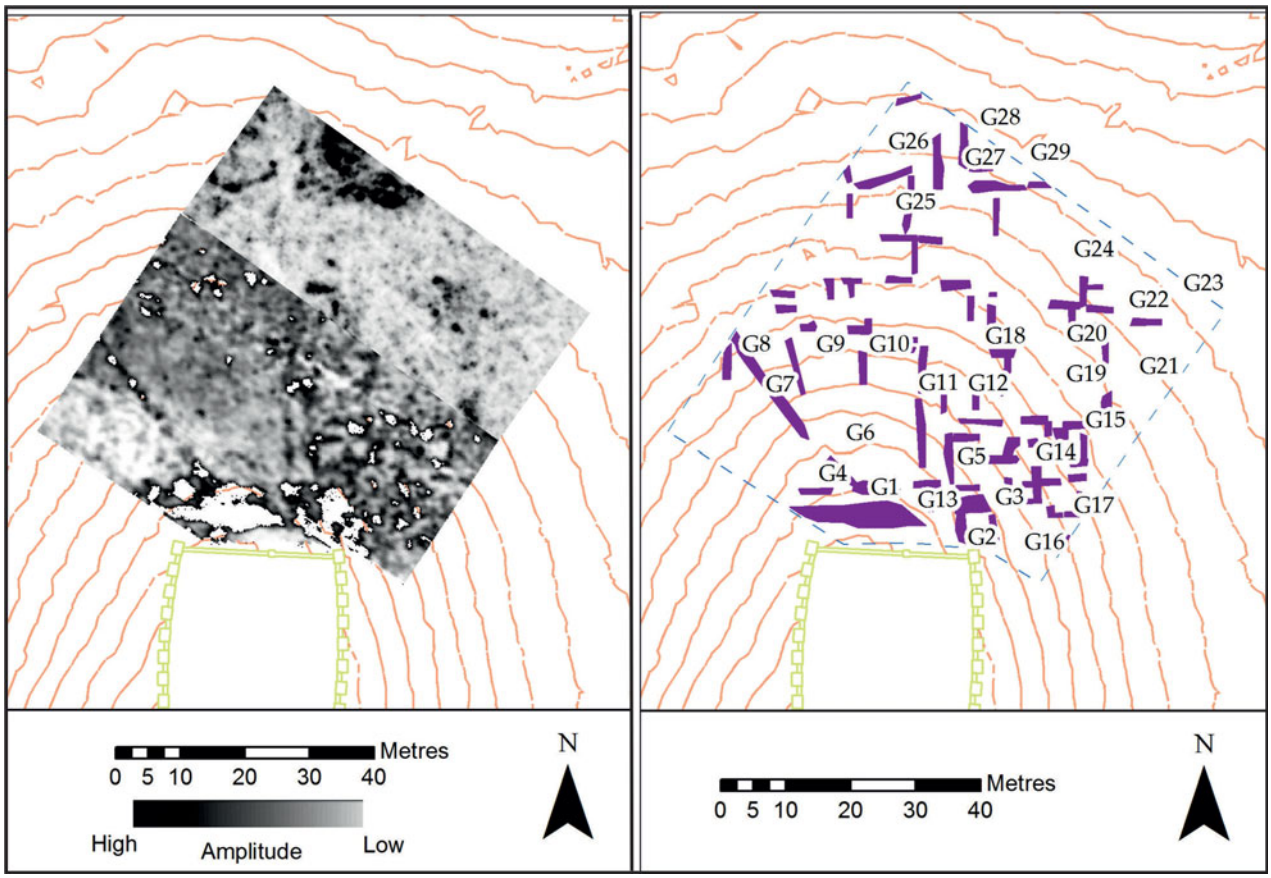

Figure 4.5. Greyscale and interpretation images of the single-antenna GPR survey results from the north of the East Mound.

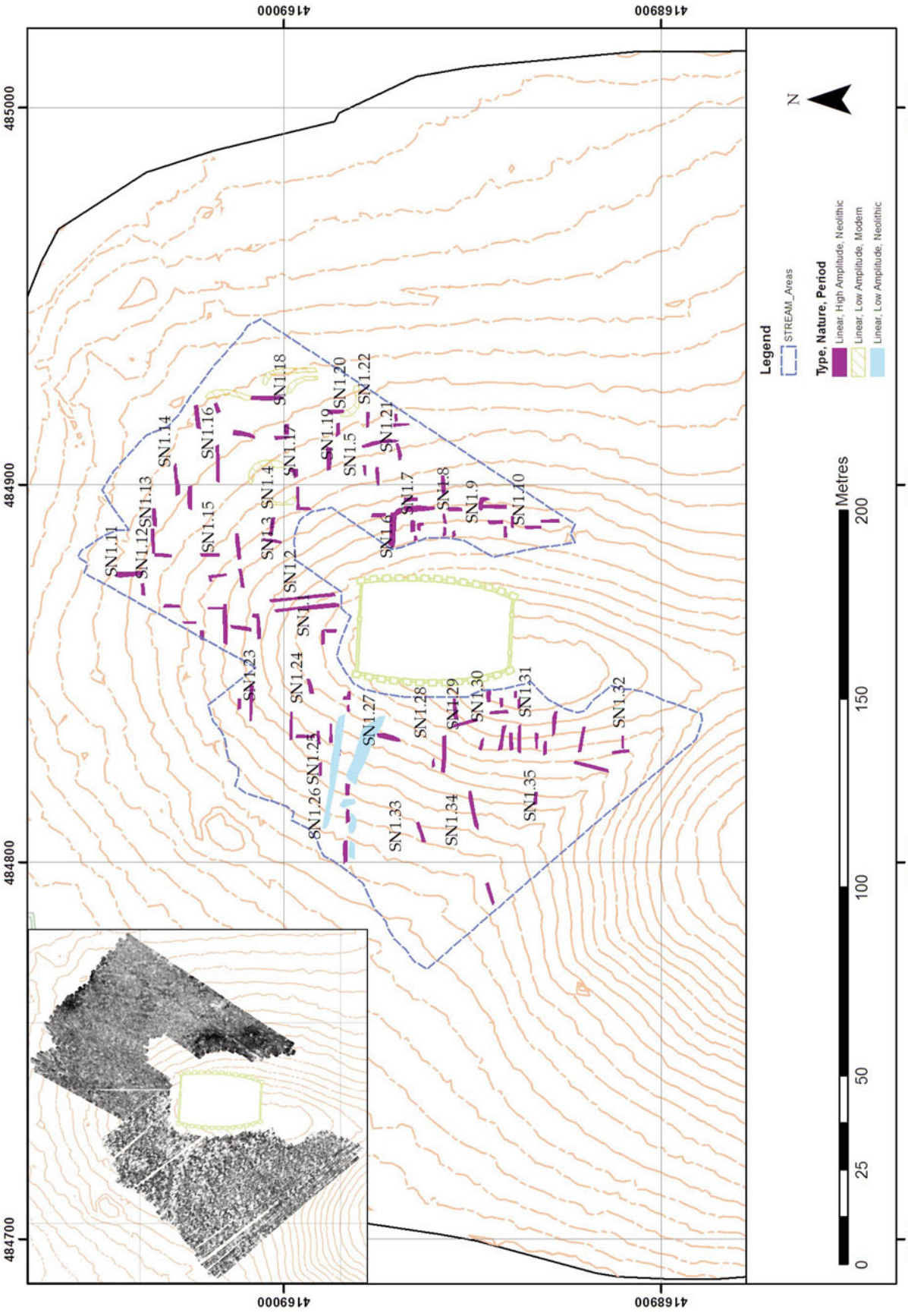

Figure 4.6. Greyscale of the STREAM results for the north part of the East Mound at 0.3–0.5m depth and interpretation plot derived from the STREAM results for the north part of the East Mound at 0.3–0.5m depth.

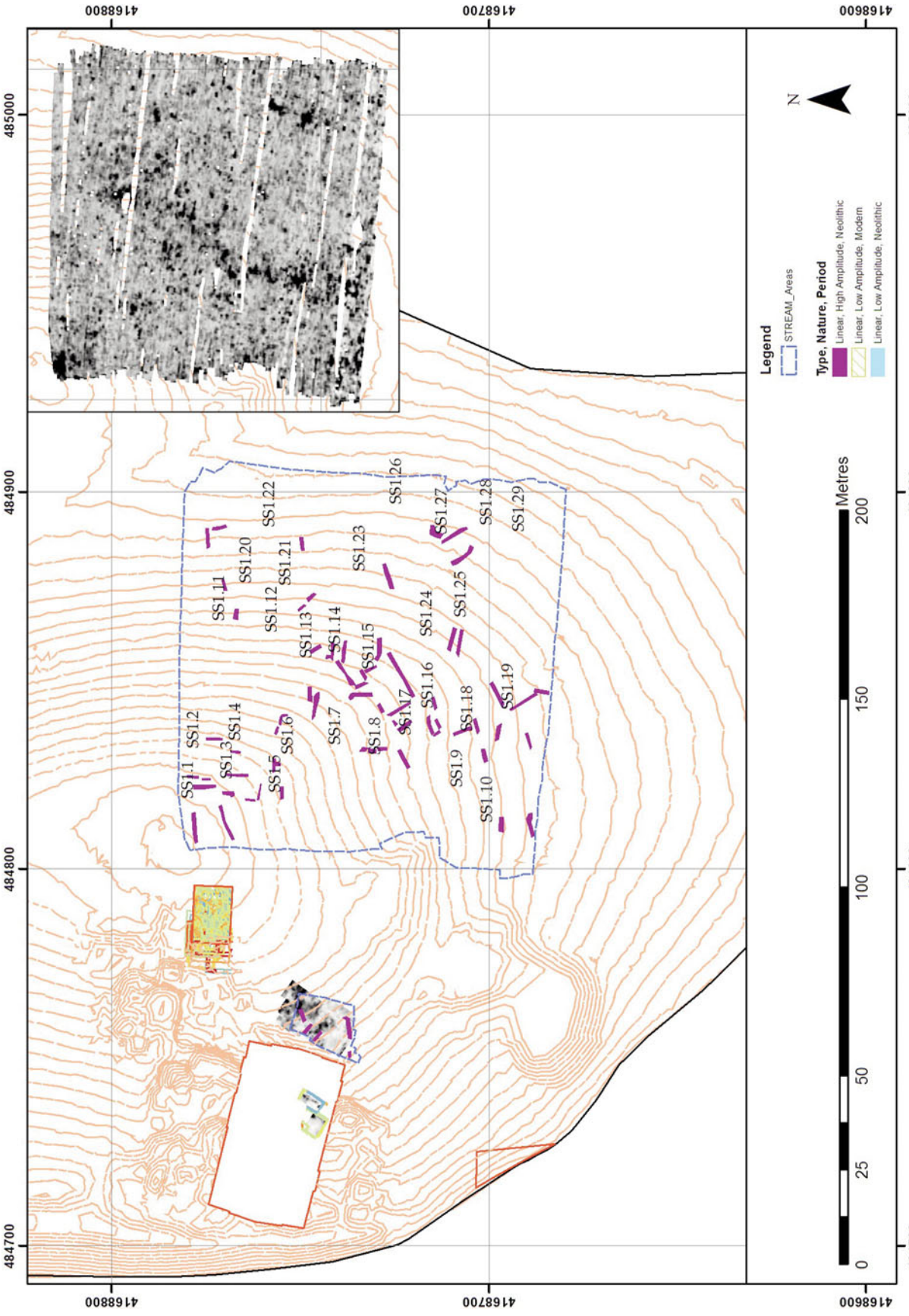

Figure 4.7. Greyscale of the STREAM results for the south part of the East Mound at 0.3–0.5m depth and interpretation plot derived from the STREAM results for the south part of the East Mound at 0.3–0.5m depth.

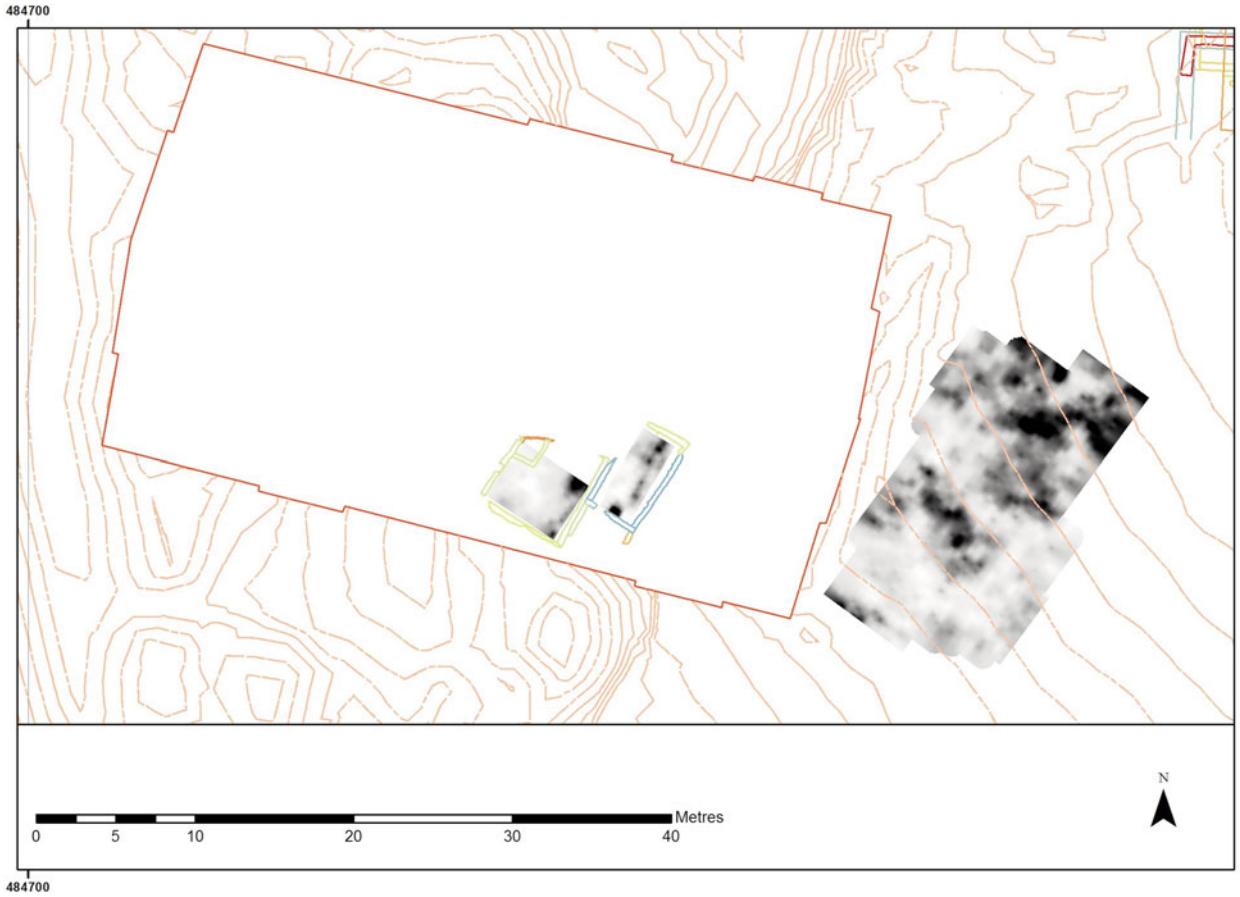

Figure 4.8. Greyscale of the GPR survey results to the east of the South Shelter and within Buildings 80 and 89 of the excavations.

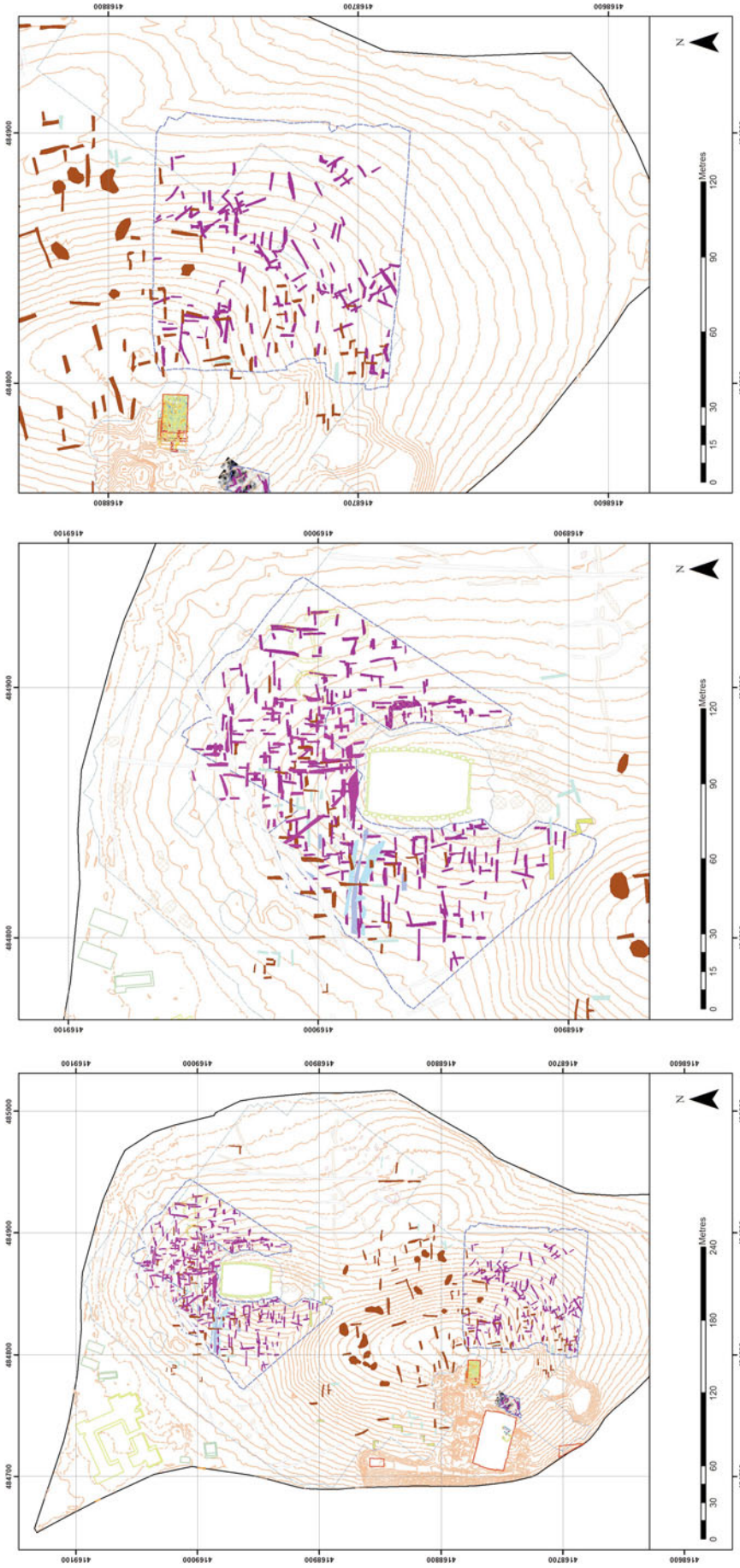

Figure 4.9. Composite plot of the magnetometer and GPR interpretations for the East Mound (left); detail of the GPR interpretations for the northern part (centre) and for the southern part of the East Mound (right).